WOOD RESEARCH doi.org/10.37763/wr.1336-4561/67.4.625635
e-ISSN 2729-8906
67(4): 2022 625-635 pp.

EMPIRICAL ANALYSIS OF ROOF SLOPE INFLUENCE ON MATERIAL CONSUMPTION IN TIMBER HOWE-TYPE TRUSSES

ISABELLA SILVA MENEZES, IURI FAZOLIN FRAGA, MATHEUS HENRIQUE MORATO DE MORAES, ANDRÉ LUIS CHRISTOFORO
FEDERAL UNIVERSITY OF SAO CARLOS
BRAZIL

FERNANDO JÚNIOR RESENDE MASCARENHAS
UNIVERSITY OF COIMBRA
PORTUGAL

RAQUEL SCHMITT CAVALHEIRO, FRANCISCO ANTONIO ROCCO LAHR
UNIVERSITY OF SAO PAULO
BRAZIL

EDUARDO CHAHUD, LUIZ ANTÔNIO MELGAÇO NUNES BRANCO
FEDERAL UNIVERSITY OF MINAS GERAIS
BRAZIL

HERISSON FERREIRA DOS SANTOS
FEDERAL INSTITUTE OF EDUCATION SCIENCE AND TECHNOLOGY OF RONDONIA
BRAZIL

(RECEIVED FEBRUARY 2022)

ABSTRACT

In Brazil, some tile manufacturers have proposed a 10% (5.5°) slope between chords to minimize timber consumption. However, after simulating 21 slopes from 7% (4°) to 27% (15°), it was discovered that the axial strengths are inversely proportional to the slope, creating overly large dimensions for the bars competing for support. The results were obtained using software developed following the guidelines specified in the revised version of the ABNT NBR 7190 (2022) standard. Finally, it was found that the minimum slope until no reinforcement is needed for the string bars is 16% (9°).

KEYWORDS: Timber structure, plane truss, timber consumption, roof slope.

INTRODUCTION

In the last decade, there have been relevant advances in the wood industry that have the raw material from planted forests, attracting the attention of a consumer market interested in ecologically correct products (Calil Neto et al. 2014). When compared to concrete and steel, wood stands out for being a renewable and sustainable source. Furthermore, it has excellent mechanical properties (Christoforo et al. 2020), with a relatively lower strength-density ratio when compared to concrete and steel (Calil Júnior and Dias 1997, Ramage et al. 2017). For these reasons, in Scandinavian countries, Canada, Japan, and the United States, there is a strong presence of timber in constructions, principally in the wood frame system, frequently applied in residential buildings in these countries (Kirkham et al. 2014, Araujo et al. 2016, Pan et al. 2019).

Nonetheless, in Brazil, the reality is different. Given the availability of abundant forest diversity in Brazil (Steege et al. 2016, 2020), its structural use has potential for expansion (Almeida et al. 2013), with applications in diversified structural systems, despite some prejudice resulting from misinformation around its optimal performance, due to its mechanical properties. Despite being well-intentioned, the workforce still makes due to arising from the empirical dimensioning (Calil Júnior et al. 2019). In this scenario, and aiming to generate subsidies that will expand the rational consumption of timber in structures, it is essential to develop works such as the one proposed here, as Brazil is inserted in a context of recovery and reinforcement of historical and current roof structures transition stage from the artisanal construction process to the prefabrication process: truss with members joined utilizing gang nail plates (GNP) (Karel'skiy et al. 2018, Isupov and Chaganov 2019). In Brazil, timber structure projects must meet ABNT NBR 7190 (1997) standard. It is currently undergoing a review process in which some different approaches have been inserted concerning the dimensioning of structural members, resulting in the project of standard ABNT NBR 7190 (2022).

Therefore, given these circumstances, the need for research and updates about the sizing and execution of wood roof structures is highlighted to enhance their use (Fraga 2020). The literature has shown that timber applied to the structural roofing system is a topic frequently studied by researchers. Numerous variables are analyzed. The stability, buckling length, and bracing of plane truss (Burdzik and Dekker 2012, Burdzik and Skorpen 2014, Sejkot et al. 2020). The structural behavior under the loading of wind on the structure (Satheeskumar et al. 2016, 2017, Navaratnam et al. 2020). The evaluation and rehabilitation of woof roofing structures (Fonte et al. 2017, Negrão 2020). The stiffness and bond behavior in flat timber trusses (Tenorio et al. 2018, Rivera-Tenorio and Moya 2019, Que et al. 2019). Cost optimization of wood roofing structures (Villar-García et al. 2019). Wooden parts' strength and rigidity capacity in lattice roof structures (Wessels and Petersen 2015).

Despite these themes, other variables can be used. Although the application of timber in roof structures is frequent in the country, it is necessary to verify the origin of certain empirical assumptions to optimize its use. For example, claiming to lessen how much wood is in roof structures, a few fiber cement roof tile manufacturers recommend using a 10% slope (5.5°) between the chords of Howe and Pratt scissors (Oliveira et al. 2019). However, this configuration can generate greater strengths on the bars, requiring increased wood consumption

and consequent irrational use of forest resources, this being an unwanted situation. One should always look for a lean structure, i. e. optimized, because it results in lower consumption of material, which contributes to a better price in the market and also decreases the exploitation of resources and environmental impacts.

Based on presented above, the objective of this study was to evaluate if the inclination of the roof influences the sizing and wood consumption, considering Howe-type trusses with 10 m span and variation of its slope (α) from 7% (4°) to 27% (15 °). The software used was iTruss developed and calibrated by Fraga (2020). It analyzes and sizes flat timber trusses following the guidelines of the new revised standard ABNT NBR 7190 (2022).

MATERIAL AND METHODS

Geometry

The Howe-type typology was chosen for the trusses because this is a typical roof geometry in symmetrical gables. The trusses were arranged to always generate structures with eight bars on the upper chords, regardless of the slope. Thus, aiming at the generation of structures that resembled the reality of execution, technical catalogs of the adopted tile were consulted. The tile chosen is the corrugated fiber-cement type (usually used in rural/industrial buildings) was consulted so that it is possible to establish some basic guidelines in the design of the geometries. Therefore, in Tab. 1 below, the values of longitudinal coverings adopted for each slope range are presented.

Tab. 1: Minimum longitudinal covering (Eternit 2020).

Sloop range	Longitudinal covering
7% ≤ i ≤ 8%	28 cm
9% ≤ i ≤ 18%	25 cm
19% ≤ i ≤ 27%	23 cm

Considering fiber cement tiles with a thickness of 6 mm and a longitudinal balance between 25 cm and 40 cm, the configuration of the bars is illustrated in Fig. 1.

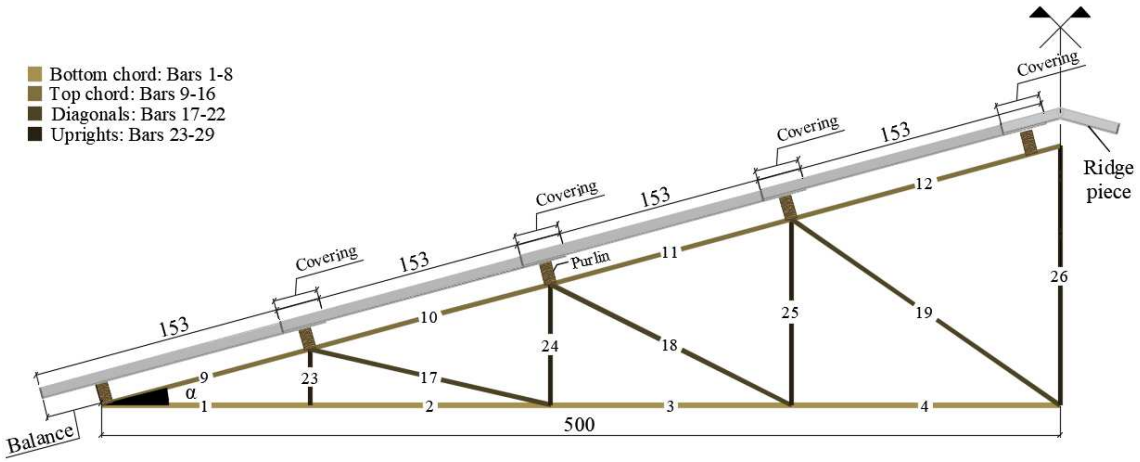

Fig. 1: Bar's configuration and shame of nodes and groups (dimensions in centimeters).

Note that for all geometries with inclinations between 7% (4°) and 27% (15°), the layout of four 153 cm roof tiles was sufficient to ensure the balance specified in the manufacturer's catalog. Therefore, in addition to resembling the design reality, the trusses vary as little as possible from each other, which allows trustworthy comparisons in the dimensioning and wood consumption generated when simulating every slope.

Loads and combinations

The truss is subject to constant loads resulting from the weight of the wooden structure and the materials used to close the roof. The loading due to dead load is not included in the iTruss software as it adapts the minimum cross-sections for each bars group and automatically updates the dead load of the structure with each iteration. It is therefore only necessary to estimate the permanent loads due to the weight of the materials attached to the structure, the value of which is approximately 0.25 $kN \cdot m^{-2}$ (weight of fiber cement roof tiles with a thickness of 6 mm = 0.18 $kN \cdot m^{-2}$; 30% by rainwater absorption = 0.054 $kN \cdot m^{-2}$; roof tiles reinforcement = 0.010 $kN \cdot m^{-2}$).

When calculating the efforts in the ultimate limit state (ULS) and displacements in the service limit states (SLS), the permanent loads were considered together, assuming the following weighting coefficients (Tab. 2, ABNT NBR 8681: 2003) for buildings type 2: γg = 1.40 for unfavorable effects (same direction as the acceleration of gravity) and γg = 1.0 for favorable effects (direction against gravity). The variable loads acting in this project are accidental loads due to the construction process (people), roof overload, and wind action. In the roofs of wooden structures, accidental loads resulting from the construction process have an intensity of 1 kN. These loads are applied to purlins and bars of the upper chords, following the orientations of item 6.4 of ABNT NBR 6120 (2019). The referred standard also prescribes that this load must be considered acting in isolation from the other variable actions in calculating the combinations, i.e., only when it is the main variable action, whose efforts are critical concerning the other combinations. On purlins, a value of 1 kN is applied in the middle of its span, a position that is unfavorable for simply-supported beams. In the upper chord bars, the equivalent uniform load method was used (Moliterno 2010). For this, a value of 1 kN is applied in each area associated with a bar on the upper chord, as illustrated in Fig. 2, with subsequent calculation of the average of all areas found. The iTruss software automatically determines this equivalent load depending on the upper chord bars' length. However, since the chords differ little from each other in each slope, the accidental load due to the construction process is assumed to be approximately 0.26 $kN \cdot m^{-2}$ for described spans and this typology.

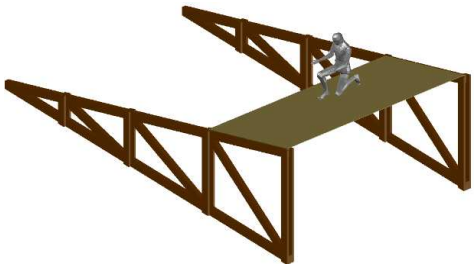

Fig. 2: Accidental construction load (people).

The revision of ABNT NBR 7190 (2022) prescribes, in its item 9.2.1, that in the absence of atypical loads, a minimum characteristic overload of 0.25 $kN \cdot m^{-2}$ of the built area must be foreseen in horizontal projection. ABNT NBR 6120 (2019) also recommends this same value in item 6.4. The wind action on the structure was determined following the ABNT NBR 6123 (2013) normative recommendations, taking into account a rectangular building (24 × 10 m), roof with symmetrical gables, and 5 m free height. The iTruss software quantifies the internal pressure and shape coefficients (Ci) by assumptions of dominant opening in different building regions, admitting perfect sealing in the meeting of the elements, not having fixed openings. However, five windows of 2.4 m^2 on each face parallel to the 0° wind were considered movable openings; a front gate of 19 m^2 and two windows of 2.4 m^2 at the back. The internal pressure and shape coefficients (Ci) were determined according to item 6.2.5 of ABNT NBR 6123 (2013) corrected and later combined with the value of dynamic wind pressure. In the ULS and SLS, the variable loads were considered separately, assuming the following coefficients (Tabs. 4-6, ABNT NBR 8681: 2003): $\gamma q = 1.50$; $\psi 0 = 0.7$; $\psi 1 = 0.6$; $\psi 2 = 0.4$ for accidental construction load and roof overload; $\gamma q = 1.40$; $\psi 0 = 0.6$; $\psi 1 = 0.3$; $\psi 2 = 0.0$ for wind action.

Structural analysis

The structural model adopted admits only bar elements (axial forces), that is, with perfectly articulated ends. In addition, the action due to dead load is discharged into the nodes of the upper chord, considering the respective areas of influence. Next, in Fig. 3, the static scheme used in all simulations is illustrated.

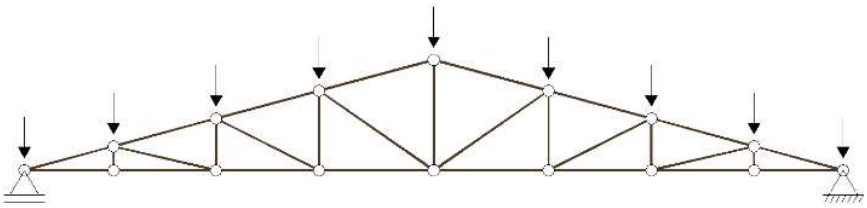

Fig. 3: Static schematic of the classic truss model.

Design

In the elements that will make up the roof purlins, timber from the hardwood group, class D40, was selected. Its characteristic resistance values ($f_{c0,k} = 40$ MPa and $f_{v0,k} = 6$ MPa), stiffness ($E_{c0,m} = 19500$ MPa) and apparent specific mass ($\rho = 9.5$ $kN.m^{-3}$) were taken from ABNT NBR 7190 (2022). For the truss bars, the type of wood adopted was also the hardwood group, however, with class D30, with resistance values ($f_{c0,k} = 30$ MPa); stiffness ($E_{c0,m} = 14500$ MPa) and apparent specific mass ($\rho = 8.0$ $kN \cdot m^{-3}$) also extracted from ABNT NBR 7190 (2022). According to the orientations of that standard, in the absence of characteristic tension strength parallel to the grain ($f_{t0,k}$) and bending strength ($f_{b,k}$), it was assumed that $f_{t0,k} = f_{b,k} = f_{c0,k}$. Furthermore, considering sawn wood, moisture class (1), and long-term loading, the value of the final modification coefficient (kmod) is 0.70 (ABNT 2022). After processing the purlins, it turned out that the typical section of 6 × 12 cm meets all verifications. Therefore, its weight is equal to 0.2052 kN (9.5*0.06*0.12*3). For this reason, at each node where there is a purlin, a point force of 0.2052 kN was applied, noting in the ridge node there are two purlins, at

this location the value of 0.4104 kN was applied. About the truss, the profiles were adopted as shown in Fig. 4 below.

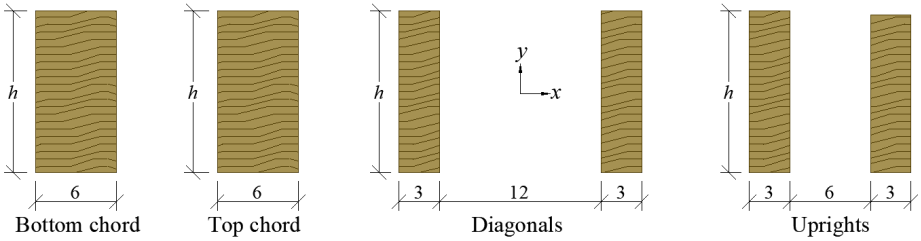

Fig. 4: Truss pieces by a group of bars (dimensions in centimeters).

Once the thickness (b) is fixed and the disposition of the parts is defined, through a repetition code with a step of 0.10 cm, the smallest height (h) whose area (A) and inertia (I) met all verification criteria is estimated. It is important to note that the load due to dead load is updated with each iteration, resulting in remarkable accuracy in the dimensions found.

RESULTS AND DISCUSSION

After the structure was processed, the wood volumes in m^3 of the truss alone were determined for each inclination (Fig. 5a). In parallel with the volume calculation, it was also decided to inform the wood consumption per unit of area in m^3/m^2 (Fig. 5b). The area under consideration results from the truss spacing (3 m) and the product between the span (10 m).

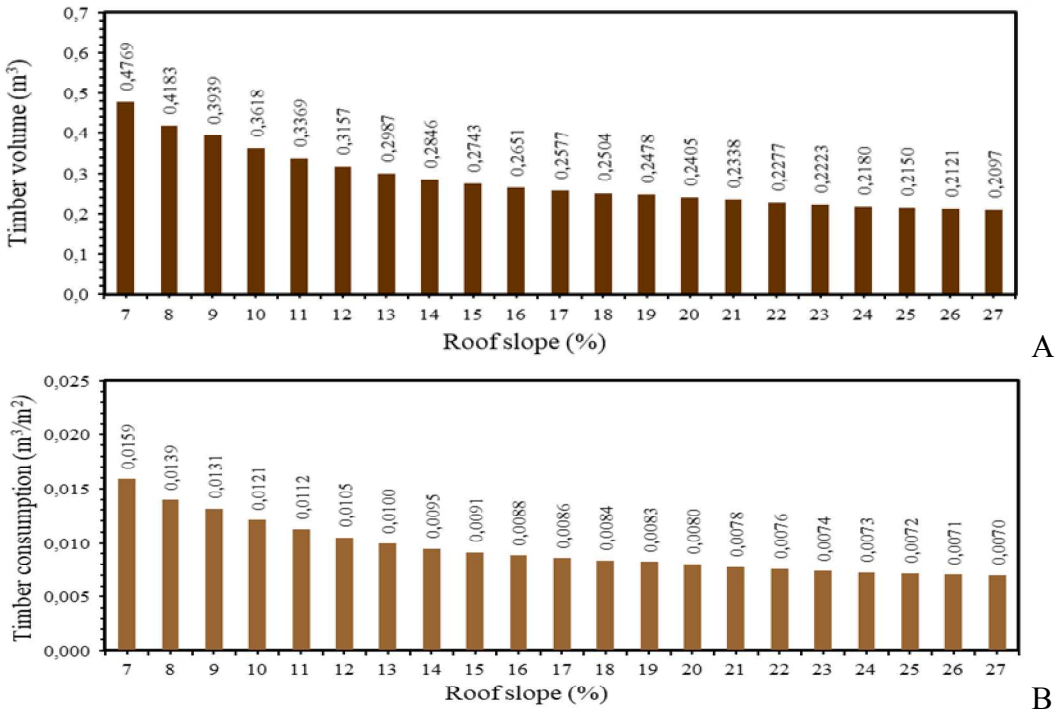

Fig. 5: a) Roof slope versus timber volume only from the truss; b) roof slope versus timber consumption only from the truss.

In order to verify the critical groups, the profiles dimensioned for the extreme slopes of 7% (4°) (Fig. 6a), and 27% (15°) (Fig. 6b) were chosen.

A

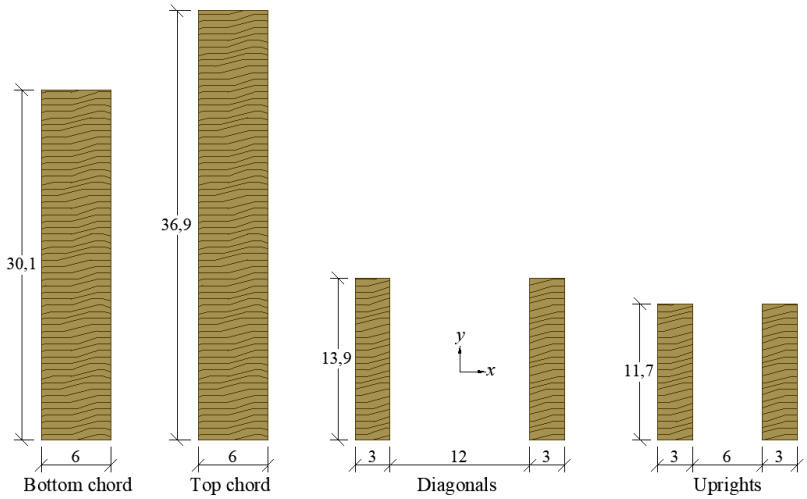

B

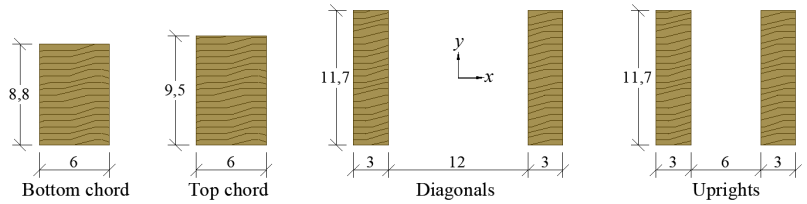

Fig. 6: Pieces designed for the slopes of: a) 7% (4°) and b) 27% (15°).

CONCLUSIONS

This work had as main objective to evaluate the influence that the roof's slope exerts on the material dimensioning and in the consumption of material in flat timber trusses. For this purpose, the iTruss software was used. It was developed and tuned by Fraga (2020) based on the sizing routine specified by revised Brazilian standard ABNT NBR 7190 (2022). By simulating 21 inclinations of a Howe-truss, with a span of 10 m, it was able to point out the following considerations: *(1)* The profiles of the uprights and diagonal bars change little due to the slope. However, the smaller the slope, the larger the dimensions of the parts that make up the chord. *(2)* The determining factor in the design was stability concerning the y-axis. Since the variation in chord bar length is minimal on each slope, when checking buckling concerning the minimum inertia axis, it is concluded that the bars compressive loads competing with the support are responsible for producing an excessive profile. *(3)* It is also concluded that, for the span and typology described, the 16% (9°) slope is the minimum value that does not require bars reinforcement are not necessary, considering that the profiles that make up the chords have very close heights the maximum commercial dimension of 16 cm (thickness fixed at 6 cm).

ACKNOWLEDGMENTS

The authors are grateful for the support of the Coordination for the Improvement of Higher Education (CAPES), the National Council for Scientific and Technological Development (CNPq) and the Federal Institute of Education, Science and Technology of Rondonia, Ariquemes Campus.

REFERENCES

1. ABNT NBR 7190, 1997: Projeto de Estruturas de Madeira (Wooden structures design).
2. ABNT NBR 7190, 2022: Projeto de Estruturas de Madeira (Wooden structures design). Revised standard.
3. ABNT NBR 6120, 2019: Ações para o cálculo de estruturas de edificações (Design loads for structures).
4. ABNT NBR 6123, 2013: Forças devidas ao vento em edificações (Building construction. Wind loads.).
5. ABNT NBR 8681, 2003: Ações e segurança nas estruturas. Procedimento (Actions and safety of structures. Procedure)
6. Almeida, D.H. de, Scaliante, R. de M., Macedo, L.B. de, Macêdo, A.N., Dias, A.A., Christoforo, A.L., Calil Junior, C., 2013: Structural characterization of the amazonian wood specie Paricá (*Schizolobium amazonicum* Herb) in members. Revista Árvore 37(6): 1175-1181.
7. Araujo, V.A. de, Cortez-Barbosa, J., Gava, M., Garcia, J.N., Souza, A.J.D. de, Savi, A.F., Morales, E.A.M., Molina, J.C., Vasconcelos, J.S., Christoforo, A.L., Lahr, F.A.R., 2016: Classification of wooden housing building systems. BioResources 11(3): 7889-7901.
8. Burdzik, W.M.G., Dekker, N.W., 2012: A rational approach to predicting the buckling length of compression chords in prefabricated timber truss roof structures braced by means of diagonal bracing. Journal of the South African Institution of Civil Engineering 54(1): 81-89.
9. Burdzik, W.M.G., Skorpen, S.A., 2014: Metal–strip bracing versus diagonal timber bracing in timber trussed tiled roofs. Engineering Structures 75: 1-10.
10. Calil Júnior, C., Dias, A.A., 1997: Utilização da madeira em construções rurais. Revista Brasileira de Engenharia Agrícola e Ambiental 1 (1): 71-77.
11. Calil Júnior, C., Lahr, F.A.R., Martins, G.C.A., Dias, A., 2019: Estruturas de madeira: Projetos, Dimensionamento e Exemplos de Cálculo (Timber structures - Projects, dimensioning and calculation examples). Elsevier. Rio de Janeiro, 208 pp.
12. Calil Neto, C., Christoforo, A.L., Ribeiro Filho, S.L.M., Lahr, F.A.R., Calil Junior, C., 2014: Evaluation of strength to shear and delamination in glued laminated wood. Ciência Florestal 24 (4): 989-996.
13. Christoforo, A.L., Almeida, D.H. de, Varanda, L.D., Panzera, T.H., Lahr, F.A.R., 2020: Estimation of wood toughness in Brazilian tropical tree species. Engenharia Agrícola 40(2): 232-237.

14. Eternit, 2020. Catálogo Técnico: Telhas de fibrocimento CRFS. Eternit. São Paulo, 118 pp.
15. Fonte, A.P.N. da, Anjos, R.A.M. dos, Kovalski, M., Oliveira, G.R. de, Bernardo, J., 2017: Structural analysis of the wooden roof of a historic building – Casa da Cultura da Colônia Murici – in São José dos Pinhais, Paraná state. Ciência Florestal 27(1): 363-375.
16. Fraga, I.F., 2020: Influência dos modelos idealizados de ligações no dimensionamento de treliças planas de madeira (Idealized joint models influence on the design of plane timber trusses). Dissertação (Mestrado em Engenharia Civil). Programa de Pós-Graduação em Engenharia Civil, Universidade Federal de São Carlos, São Carlos, 91 pp.
17. Isupov, S.A., Chaganov, A.B., 2019: Strength and stiffness of wood structures for compounds of gang nail plate "Steelcap". IOP Conference Series: Materials Science and Engineering 687(3): 033015.
18. Karel'skiy, A.V., Zhuravleva, T.P., Filippov, V.V., Labudin, B.V., Melekhov, V.I., 2018: Reinforcement technology of laminated wood structures by gang nail. Lesnoi Zhurnal 1: 80-88.
19. Kirkham, W.J., Gupta, R., Miller, T.H., 2014: State of the art: Seismic behavior of wood-frame residential structures. Journal of Structural Engineering 140(4): 04013097.
20. Moliterno, A., 2010: Caderno de Projetos de Telhados em Estruturas de Madeira (Notebook of roofing projects in wooden structures). Blucher. São Paulo, 284 pp.
21. Navaratnam, S., Ginger, J., Humphreys, M., Henderson, D., Wang, C.-H., T.Q. Nguyen, K., Mendis, P., 2020: Comparison of wind uplift load sharing for Australian truss- and pitch-framed roof structures. Journal of Wind Engineering and Industrial Aerodynamics 204: 104246.
22. Negrão, J.H., 2020: Rehabilitation of the roof timber trusses of a multiuse pavilion. Civil Engineering Journal 6(12): 2437-2447.
23. Oliveira, G.O.B., Pinheiro, R.V., Arroyo, F.N., Almeida, D.H. de, Almeida, T.H. de, Silva, D.A.L., Christoforo, A.L., Lahr, F.A.R., 2019: Technical feasibility study of the use of softwoods in lattice structure "Howe" type for roofing (gaps between 8-18 meters). Current Journal of Applied Science and Technology, Pp 1-8.
24. Pan, Y., Ventura, C.E., Finn, W.D.L., Xiong, H., 2019: Effects of ground motion duration on the seismic damage to and collapse capacity of a mid-rise wood frame building. Engineering Structures 197: 109451.
25. Que, Z., Hou, T., Gao, Y., Teng, Q., Chen, Q., Wang, C., Chang, C., 2019: Influence of Different Connection Types on Mechanical Behavior of Girder Trusses. Journal of Bioresources and Bioproducts 4(2): 89-98.
26. Ramage, M.H., Burridge, H., Busse-Wicher, M., Fereday, G., Reynolds, T., Shah, D.U., Wu, G., Yu, L., Fleming, P., Densley-Tingley, D., Allwood, J., Dupree, P., Linden, P.F., Scherman, O., 2017: The wood from the trees: The use of timber in construction. Renewable and Sustainable Energy Reviews 68: 333-359.
27. Rivera-Tenorio, M., Moya, R., 2019: Stress, displacement joints of *Gmelina arborea* and *Tectona grandis* wood with metal plates, screws and nails for use in timber truss connections. Cerne 25(2): 172-183.

28. Satheeskumar, N., Henderson, D.J., Ginger, J.D., Humphreys, M.T., Wang, C.H., 2016: Load sharing and structural response of roof-wall system in a timber-framed house. Engineering Structures 122: 310-322.
29. Satheeskumar, N., Henderson, D.J., Ginger, J.D., Wang, C.-H., 2017: Three-dimensional finite-element modeling and validation of a timber-framed house to wind loading. Journal of Structural Engineering 143(9): 04017112.
30. Sejkot, P., Ormarsson, S., Vessby, J., Källsner, B., 2020: Numerical out-of-plane stability analysis of long span timber trusses with focus on buckling length calculations. Engineering Structures 204: 109670.
31. Steege, H. ter, Prado, P.I., Lima, R.A.F. de, Pos, E., de Souza Coelho, L., de Andrade Lima Filho, D., et al., 2020: Biased-corrected richness estimates for the Amazonian tree flora. Scientific Reports 10(1): 10130.
32. Steege, H. ter, Vaessen, R.W., Cárdenas-López, D., Sabatier, D., Antonelli, A., de Oliveira, S.M., Pitman, N.C.A., Jørgensen, P.M., Salomão, R.P., 2016: The discovery of the Amazonian tree flora with an updated checklist of all known tree taxa. Scientific Reports 6(1): 29549.
33. Tenorio, C., Moya, R., Carranznza, M., Navarro, A., Saenznz, M., Paniagua, V., 2018: Mechanical performance in flexure for two spans of trusses from *Hieronyma alchorneoides* and *Gmelina arborea* woods fastened with nails and screws. Journal of Tropical Forest Science 30(3): 330-341.
34. Villar-García, J.R., Vidal-López, P., Rodríguez-Robles, D., Guaita, M., 2019: Cost optimisation of glued laminated timber roof structures using genetic algorithms. Biosystems Engineering 187: 258-277.
35. Wessels, C.B., Petersen, N.O., 2015: Strength and stiffness capacity utilisation of timber members in roof truss structures. Southern Forests: a Journal of Forest Science 77(4): 305-307.

ISABELLA SILVA MENEZES*, IURI FAZOLIN FRAGA, MATHEUS HENRIQUE MORATO DE MORAES, ANDRÉ LUIS CHRISTOFORO
FEDERAL UNIVERSITY OF SAO CARLOS – SÃO CARLOS
DEPARTMENT OF CIVIL ENGINEERING
RODOVIA WASHINGTON LUÍS – 36.307-352
SÃO CARLOS
BRAZIL
*Corresponding author: ec.isabellasm@gmail.com

FERNANDO JÚNIOR RESENDE MASCARENHAS
UNIVERSITY OF COIMBRA
RUA SÍLVIO LIMA, UC – POLO II - 3030-790
COIMBRA
PORTUGAL

RAQUEL SCHMITT CAVALHEIRO, FRANCISCO ANTONIO ROCCO LAHR
UNIVERSITY OF SAO PAULO – SÃO CARLOS
DEPARTMENT OF STRUCTURAL ENGINEERING
AV. TRABALHADOR SÃOCARLENSE, N. 400 – 13.566-590
SÃO CARLOS
BRAZIL

EDUARDO CHAHUD, LUIZ ANTÔNIO MELGAÇO NUNES BRANCO
FEDERAL UNIVERSITY OF MINAS GERAIS – BELO HORIZONTE
DEPARTMENT OF CIVIL ENGINEERING
AV. ANTÔNIO CARLOS, N. 6627 – 31.270-901
BELO HORIZONTE
BRAZIL

HERISSON FERREIRA DOS SANTOS
FEDERAL INSTITUTE OF EDUCATION SCIENCE AND TECHNOLOGY OF RONDONIA – ARIQUEMES
DEPARTMENT OF MATERIAL ENGINEERING
AV. JUSCELINO KUBITSCHEK, N. 2717 A 2853 – 76.872-847
ARIQUEMES
BRAZIL